Dopamine Interaction in the Absence and in the Presence of Cu^{2+} Ions with Macrocyclic and Macrobicyclic Polyamines Containing Pyrazole Units. Crystal Structures of $[Cu_2(\mathbf{L}_1)(H_2O)_2](ClO_4)_4$ and $[Cu_2(H_{-1}\mathbf{L}_3)](ClO_4)_3 \cdot 2H_2O$

Laurent Lamarque,[†] Pilar Navarro,*[,†] Carlos Miranda,[†] Vicente J. Arán,[†] Carmen Ochoa,[†] Francisco Escartí,[‡] Enrique García-España,*[,‡] Julio Latorre,[‡] Santiago V. Luis,[§] and Juan F. Miravet[§]

Contribution from Instituto de Química Médica, Centro de Química Orgánica Manuel Lora Tamayo, CSIC, Juan de la Cierva 3, 28006 Madrid, Spain, Departamento de Química Inorgánica, Facultad de Química, Universitat de València, c/ Doctor Moliner 50, 46100 Burjassot (València), Spain, and Departamento de Química Inorgánica y Orgánica, Universitat Jaume I, Carretera Borriol s/n, Castellón, Spain

Received April 13, 2001

Abstract: The interaction with Cu^{2+} and dopamine of three polyazacyclophanes containing pyrazole fragments as spacers is described. Formation of mixed complexes Cu^{2+}−macrocycle−dopamine has been studied by potentiometric methods in aqueous solution. The crystal structures of the complexes $[Cu_2(\mathbf{L}_1)(H_2O)_2](ClO_4)_4 \cdot 2H_2O$ (**4**) ($\mathbf{L}_1$ = 13,26-dibenzyl-3,6,9,12,13,16,19,22,25,26-decaazatricyclo[22.2.1.1^{11,14}]octacosa-1(27),11,14(28),24-tetraene) and $[Cu_2(H_{-1}\mathbf{L}_3)](HClO_4)(ClO_4)_2 \cdot 2H_2O$ (**6**) ($\mathbf{L}_3$ = 1,4,7,8,11,14,17,20,21,24,29,32,33,36-tetradecaazapentacyclo[12.12.12.1^{6,9}.1^{19,22}.1^{31,34}]hentetraconta-6,9(41),19(40),21,31,34(39)-hexaene) are presented. In the first one (**4**), each Cu^{2+} coordination site is made up by the three nitrogens of the polyamine bridge, a sp^2 pyrazole nitrogen and one water molecule that occupies the axial position of a square pyramid. The distance between the copper ions is 6.788(2) Å. In the crystal structure of **6**, the coordination geometry around each Cu^{2+} is square pyramidal with its base being formed by two secondary nitrogens of the bridge and two nitrogen atoms of two different pyrazolate units which act as exobidentate ligands. The axial positions are occupied by the bridgehead nitrogen atoms; the elongation is more pronounced in one of the two sites [Cu(1)−N(1), 2.29(2) Å; Cu(2)−N(6), 2.40(1) Å]. The Cu−N distances involving the deprotonated pyrazole moieties are significantly shorter than those of the secondary nitrogens. The Cu(1)···Cu(2) distance is 3.960(3) Å. The pyrazole in the noncoordinating bridge does not deprotonate and lies to one side of the macrocyclic cavity. One of the aliphatic nitrogens of this bridge is protonated and hydrogen bonded to a water molecule, which is further connected to the sp^2 nitrogen of the pyrazole moiety through a hydrogen bond. The solution studies reveal a ready deprotonation of the pyrazole units induced by coordination to Cu^{2+}. In the case of $\mathbf{L}_2$ ($\mathbf{L}_2$ = 3,6,9,12,13,16,19,22,25,26-decaazatricyclo[22.2.1.1^{11,14}]octacosa-1(27),11,14(28),24-tetraene), deprotonation of both pyrazole subunits is already observed at pH ca. 4 for 2:1 Cu^{2+}:$\mathbf{L}_2$ molar ratios. All three free receptors interact with dopamine in aqueous solution. $\mathbf{L}_3$ is a receptor particularly interesting with respect to the values of the interaction constants over five logarithmic units at neutral pH, which might suggest an encapsulation of dopamine in the macrocyclic cage. All three receptors form mixed complexes Cu^{2+}−**L**−dopamine. The affinity for the formation of ternary dopamine complexes is particularly high in the case of the binuclear Cu^{2+} complexes of the 1-benzyl derivative $\mathbf{L}_1$.

Introduction

Supramolecular chemistry bases its progress in the design of highly organized molecular receptors able to discriminate and/or induce characteristic properties in given substrates.[1] Among the wealth of molecules that can be the target of recognition, neurotransmitter catecholamines are particularly interesting due to their many biological implications. Concretely, dopamine is involved in the normal emotional and autonomic control of humans. The physiological level of dopamine is altered in neurodegenerative and mental illnesses as well as in toxic syndromes induced by cocaine and psychotropic drugs.[2] Therefore receptors able to modulate the dopamine level by selective complexation or transport mechanisms represents a research goal of great interest.

In this respect, azacyclophanes containing pyrazole spacers can be adequate candidates since, apart from disposing of polyamine sites able to coordinate a variety of guests, their own pyrazole spacer may cooperate in the recognition event. Polyamine receptors can behave as ambivalent receptors since

[†] CSIC.

[‡] Universitat de València.

[§] Universitat Jaume I.

(1) Lehn, J.-M. *Angew. Chem., Int. Ed. Engl.* **1988**, *27*, 89. Lehn, J.-M. *Supramolecular Chemistry, Concepts and Perspectives*; VCH: Weinheim, Germany, 1995.

(2) (a) Nestler, E. J. *J. Neurosci.* **1992**, *12*, 2439. (b) Giros, B.; Jaber, M.; Jones, R. S.; Wightman, R. M.; Caron, M. G. *Nature* **1996**, *379*, 606. Hoffman, B. B.; Lefkowitz, R. J. In *The Pharmacological Basis of Therapuetics*; Hardman J. G., Limbird, L., Eds.; Goodmas & Gilman's, McGraw-Hill: New York, 1996; Chapter 10.

10.1021/ja010956p CCC: $20.00
Published on Web 10/09/2001

Scheme 1

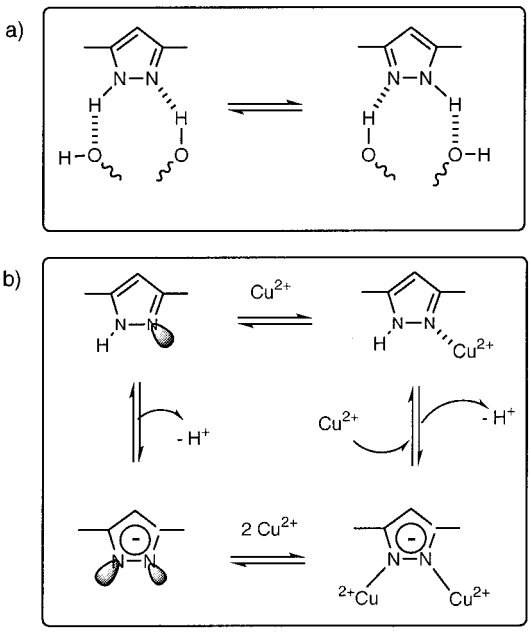

their partly or fully protonated forms can interact electrostatically or/and through hydrogen bonds with anionic or polar substrates such as catechol while, when deprotonated and, thus, disposing of free lone pairs, they can interact with metal ions acting as Lewis bases.[3,4]

With respect to dopamine coordination, the pyrazole unit may participate in the binding donating or accepting hydrogen bonds through its NH or its sp^2 N groups, respectively (Scheme 1a). On the other hand, the neutral pyrazole unit can provide coordinative bonds to metal ions as an electron donor through the sp^2 nitrogen atom. When pyrazole deprotonates to give the pyrazolate anion, it can also act as a bridging ligand between metal centers (Scheme 1b).[5,6]

Another possible coordination mode results from the use of either coordinatively unsaturated metal complexes or metal complexes with labile ligands in their first coordination sphere. These metal complexes behave as Lewis acids and may coordinate different substrates as exogenous ligands, giving rise to the formation of mixed or ternary complexes. Dopamine is a good candidate for this type of recognition due to the high strength of the catechol−copper(II) bonds and to the relevance of such complexes in biology.[7,8]

Previously, we reported on the synthesis of 13,26-dibenzyl-3,6,9,12,13,16,19,22,25,26-decaazatricyclo[22.2.1.$1^{11,14}$]octacosa-1(27),11,14(28),24-tetraene (**L**$_1$), 3,6,9,12,13,16,19,22,25,26-decaazatricyclo[22.2.1.$1^{11,14}$]octacosa-1(27),11,14(28),24-tetraene (**L**$_2$), and the cryptand 1,4,7,8,11,14,17,20,21,24,29,32,33,36-tetradecaazapentacyclo[12.12.12.$1^{6,9}$.$1^{19,22}$.$1^{31,34}$]hentetraconta-6,9(41),19(40),21,31,34(39)-hexaene (**L**$_3$), as well as on the protonation behavior of **L**$_1$ and **L**$_2$.[9−11]

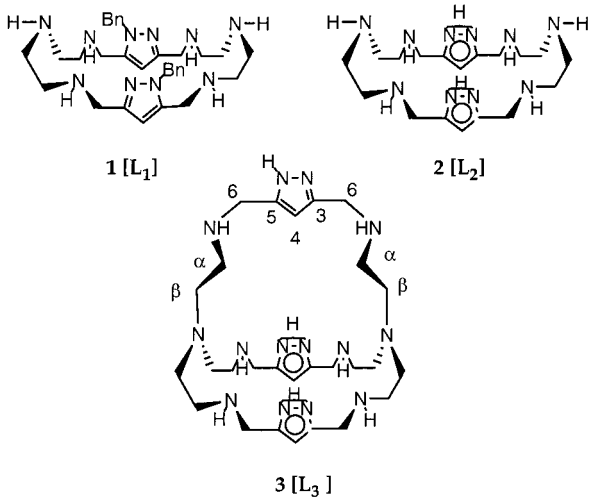

It was demonstrated that **L**$_1$ and **L**$_2$ present six protonation steps in aqueous solution that correspond to the number of nitrogen atoms in the polyamine bridges and that in the pH range 2−11 the pyrazole rings were not involved in protonation or deprotonation processes. On the other hand, a careful ^{1}H and ^{13}C NMR study of the 1-benzyl substituted receptor **L**$_1$ proved that its structure corresponds to a unique conformational isomer with the benzyl substituents located each other in opposite position.[11] Additionally, some of us have also presented the crystal structures of a binuclear Cu^{2+} complex of **L**$_1$ in which the pyrazole moieties were deprotonated acting as exobidentate ligands.[12]

In the present work we explore the capabilities of receptors **L**$_1$, **L**$_2$, and **L**$_3$ to coordinate Cu^{2+} and to interact with dopamine in aqueous solution, both in the absence and in the presence of Cu^{2+} ions. We show as Cu^{2+} coordination induces the ready deprotonation of the 1H-pyrazole rings at remarkably low pH values and how **L**$_3$ seems to be a particularly well-suited receptor for the recognition of dopamine in water. Additionally, we present the crystal structures of the complexes $[Cu_2(\mathbf{L}_1)(H_2O)_2](ClO_4)_4 \cdot 2H_2O$ and $[Cu_2(H_{-1}\mathbf{L}_3)(ClO_4)_3] \cdot 2H_2O$. (Some of these results have been advanced in the following: Lamarque, L.; Miranda, C.; Navarro, P.; Escartí, F.; García-España, E.; Latorre, J.; Ramírez, J. A. *Chem. Commun.* **2000**, 1337.)

Results and Discussion

Dopamine Recognition. Our first objective was the study of the interaction of receptors **L**$_1$−**L**$_3$ with dopamine in aqueous solution. In Table 1 are presented the stability constants for the

(3) For a general reference on anion coordination chemistry: *Supramolecular Chemistry of Anions*; Bianchi, A., Bowman-James, K., García-España, E., Eds.; John Wiley & Sons: New York, 1997. Some selected references may be: (a) Kimura, E.; Watanabe, A.; Kodama, M. *J. Am. Chem. Soc*. **1983**, *105*, 2063. (b) Kimura, E. *Top. Curr. Chem.* **1985**, *128*, 113. (c) Kimura, E.; Fujioka, H.; Kodama, M. *J. Chem. Soc., Chem. Commun.* **1986**, 1158. (d) Kimura, E.; Kuramoto, Y.; Koike, T.; Fijioka, H. Kodama, M. *J. Org. Chem.* **1990**, *55*, 42 and references cited therein. (e) Llobet, A.; Reibenspies, J.; Martell, A. E. *Inorg. Chem.* **1994,** *33*, 5946. (f) Aguilar, J. A.; García-España, E.; Guerrero, J. A.; Luis, S. V.; Llinares, J. M.; Miravet, J. F.; Ramirez, J. A.; Soriano, C. *J. Chem. Soc., Chem. Commun.* **1995**, 2237.

(4) See for instance: Bianchi, A.; Micheloni, M.; Paoletti, P. *Coord. Chem. Rev.* **1991**, *110*, 17.

(5) Elguero, J. Pyrazoles. In *Comprehensive Heterocyclic Chemistry II, A Review of the Literature 1982−1995*; Katritzky, A. R., Rees C. V., Scriven, E. F. V., Eds.; 1997; Vol. 3.

(6) Mukherjee, R. *Coord. Chem. Rev.* **2000**, *203*, 151.

(7) (a) Sigel, H. *Angew. Chem, Int. Ed. Engl.* **1975**, *14*, 394. (b) Gergerly, A.; Kiss, T.; Deak. G. *Inorg. Chim. Acta* **1979**, *36*, 113. (c) Bol. J. E.; Maase, B.; Gonesh, G.; Dreiessen, W. L.; Goubuttz, K.; Reedijk, J. *Heterocycles* **1997**, *45*, 1447. Bol. J. E.; Driessen, W. L.; Ho, Y. N.; Maase, B.; Que, L.; Reedijk, J. *Angew. Chem., Int. Ed. Engl.* **1997**, *36*, 998.

(8) Solomon, E.; Sundaram, U. M.; Machonkin, T. E. *Chem. Rev.* **1996**, *96*, 2563.

(9) Kumar, M.; Arán, V. J.; Navarro, P. *Tetrahedron Lett.* **1993**, *34*, 3159.

(10) Kumar, M.; Arán, V. J.; Navarro, P. *Tetrahedron Lett.* **1995**, *36*, 2161.

(11) Arán. V. J.; Kumar, M.; Molina, J.; Lamarque, L.; Navarro, P.; García-España, E.; Ramírez, J. A.; Luis, S. V.; Escuder, B. *J. Org. Chem.* **1999**, *64*, 6135.

(12) Kumar, M.; Arán, V. J.; Navarro, P.; Ramos-Gallardo, A.; Vegas, A. *Tetrahedron Lett*. **1994**, *35*, 5723.

Table 1. Equilibrium Constants for the Interaction of Dopamine with the Receptors $\mathbf{L}_1$, $\mathbf{L}_2$, and $\mathbf{L}_3$ Determined in 0.15 mol dm^{-3} NaCl at 298.1 K

entry	reaction[a]	$\mathbf{L}_1$	$\mathbf{L}_2$	$\mathbf{L}_3$
1	Do + **L** + H ⇌ H(Do)**L**			16.19(2)
2	Do + 2H + **L** ⇌ H_2(Do)**L**			25.72(2)
3	Do + 3H + **L** ⇌ H_3(Do)**L**	31.16(8)	32.08(4)	34.57(2)
4	Do + 4H + **L** ⇌ H_4(Do)**L**	39.42(6)	40.71(3)	43.04(2)
5	Do + 5H + **L** ⇌ H_5(Do)**L**	46.49(6)	48.13(4)	50.39(2)
6	Do + 6H + **L** ⇌ H_6(Do)**L**	52.52(6)	55.51(4)	57.08(2)
7	Do + 7H + **L** ⇌ H_7(Do)**L**	56.38(7)	59.96(6)	63.40(2)
8	Do + 8H + **L** ⇌ H_8(Do)**L**	59.72(6)	63.04(7)	
9	HDo + **L** ⇌ H(Do)**L**			5.8
10	HDo + H**L** ⇌ H_2(Do)**L**			5.9
11	HDo + H_2**L** ⇌ H_3(Do)**L**	3.6	3.1	6.0
12	H_2Do + H**L** ⇌ H_3(Do)**L**	3.1	3.1	5.8
13	H_2Do + H_2**L** ⇌ H_4(Do)**L**	3.0	2.9	5.6
14	H_2Do + H_3**L** ⇌ H_5(Do)**L**	3.4	2.9	5.3
15	H_2Do + H_4**L** ⇌ H_6(Do)**L**	3.6	2.9	5.2
16	H_2Do + H_5**L** ⇌ H_7(Do)**L**	3.8	2.8	5.4
17	H_2Do + H_6**L** ⇌ H_8(Do)**L**	5.0	2.7	

[a] Charges omitted for clarity. [b] Values in parentheses are standard deviations in the last significant figure.

Table 2. Protonation Constants of Receptors $\mathbf{L}_1$−$\mathbf{L}_3$ Determined in 0.15 mol dm^{-3} NaCl at 298.1 K

reaction	$\mathbf{L}_{1a}$	$\mathbf{L}_{2a}$	$\mathbf{L}_3$
H + **L** ⇌ H**L**[b]	8.90	9.74	9.54(2)[c]
H + H**L** ⇌ H_2**L**	8.27	8.86	8.71(1)
H + H_2**L** ⇌ H_3**L**	6.62	7.96	7.72(2)
H + H_3**L** ⇌ H_4**L**	5.85	6.83	6.55(3)
H + H_4**L** ⇌ H_5**L**	3.37	4.57	6.51(3)
H + H_5**L** ⇌ H_6**L**	2.27	3.19	5.22(3)

[a] Taken from ref 11. [b] Charges omitted for clarity. [c] Values in parentheses are standard deviations in the last significant figure.

Scheme 2

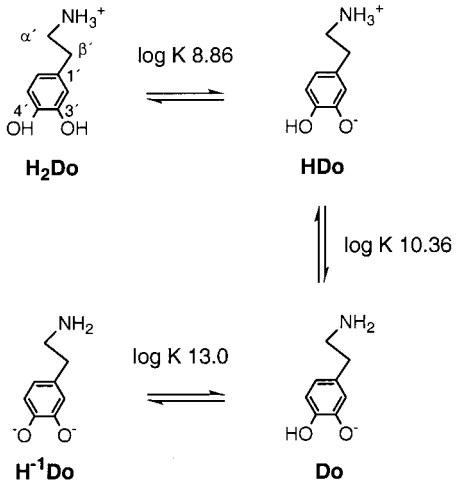

formation of the different adducts dopamine−receptor determined by pH-metric titration in the pH range 2.5−9.0. A step required for obtaining the adduct stability constants is the previous determination of the protonation constants of receptors and substrate under the same experimental conditions. The values for such constants are included in Table 2 and Scheme 2, respectively.

The stoichiometries derived from the analysis of the potentiometric data are always 1:1 receptor:dopamine. $\mathbf{L}_1$ and $\mathbf{L}_2$ form dopamine adducts with protonation degrees that vary between 3 ([H_3**L**Do]$^{2+}$ species) and 8 ([H_8**L**Do]$^{7+}$ species), while for $\mathbf{L}_3$ the protonation degrees change from 1 to 8 ([H$\mathbf{L}_3$Do] and [$H_8\mathbf{L}_3$Do]$^{7+}$ species) throughout the pH range explored (pH 2.5−9.5). At physiological pH the average protonation degree of the adducts formed is around 5 in all three systems. However, the protonation degrees achieved by the different systems deserve some comment. First of all, to understand the actual distribution of protons between receptor and substrate, the protonation constants of the receptors and of dopamine have to be evaluated. We define "Do" as the mononegatively charged species in which the amino group and one of the hydroxyl groups are deprotonated. The protonation of the amino group in our experimental conditions to give HDo presents log $K_{\mathrm{HDo/H.Do}} = 10.36$, and the protonation of the phenolate group to yield the positively charged H_2Do^+ species has log $K_{\mathrm{H_2Do/HDo.H}} = 8.86$ (see Scheme 2). Therefore, in view of these values H_2Do^+ is the prevalent species at pH 7.4, and this also has to be the situation in the binary system receptor−dopamine, unless the interaction with the receptors dramatically changes the acidity of dopamine, which is not the case of the systems here reported.

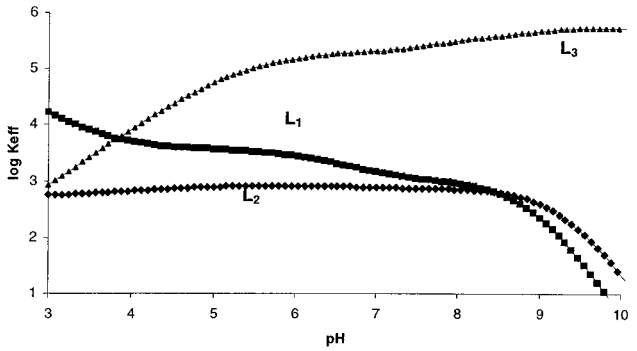

Figure 1. Plot of the logarithms of the conditional constants (K_{eff}) vs pH for the systems $\mathbf{L}_1$−Do, $\mathbf{L}_2$−Do, and $\mathbf{L}_3$−Do.

Therefore, taking into account this consideration and the protonation constants of the receptors (Table 2), the species [H_5LDo]$^{4+}$ should be the result of the reaction between H_2Do^+ and H_3L^{3+}, and the [H_6LDo]$^{5+}$ product, of the reaction of H_2Do^+ and H_4L^{4+}. The same reasoning shows that HDo is the intervening species in the formation of the mono- and diprotonated adducts. With all these considerations in mind, the overall association constants can be simplified to the stepwise constants shown at the bottom of Table 1. However, this analysis is not so straightforward for the species with intermediate protonation degrees (3 and 4), and several equilibria can simultaneously contribute to the formation of a given adduct. Therefore, to avoid any misinterpretation of the selectivity patterns due to an erroneous consideration of the basicity of receptor and substrate, it is convenient to define for each pH value an effective stability constant as the quotient between the overall amounts of complexed dopamine and those of noncomplexed dopamine and ligand.[13]

$$\log K_{\mathrm{eff}} = \sum[(\mathrm{H}_i\mathrm{Do})(\mathrm{H}_j\mathrm{L})]/\{\sum[\mathrm{H}_j\mathrm{L}]\sum[\mathrm{H}_i\mathrm{Do}]\}$$

A plot of the logarithms of the stability constants vs pH confirms that the $\mathbf{L}_3$ adducts prevail over those of $\mathbf{L}_1$ and $\mathbf{L}_2$ and permits one to establish selectivity ratios at any pH value by dividing the values of the effective constants (Figure 1). It is interesting to note that the profile of the log K_{eff} vs pH curve for $\mathbf{L}_3$ showing an increase of the constant with the pH, is opposite those of $\mathbf{L}_1$ and $\mathbf{L}_2$.

(13) (a) Bianchi, A.; García-España, E. *J. Chem. Educ.* **1999**, *12*, 1727. (b) Aguilar, J. A.; Celda, B.; Fusi, V.; García-España, E.; Luis, S. V.; Martínez, M. C.; Ramírez, J. A.; Soriano, C.; Tejero, B. *J. Chem. Soc., Perkin Trans. 2* **2000**, 1323.

Chart 1

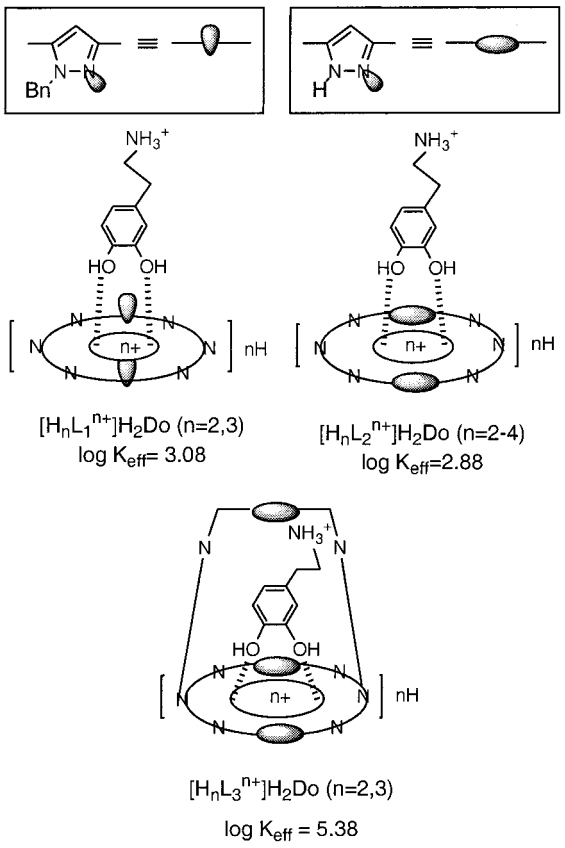

It is also remarkable that, particularly for $\mathbf{L}_3$, there is not a direct correlation between the charge of the receptor and the strength of the interaction. This might be an indication of the importance that forces other than charge−charge or charge−dipole interaction may have in these systems. To achieve a maximum interaction, a certain degree of conformational freedom is needed in order to rightly arrange the functionalities of receptor and substrate, and thereby a high protonation degree of the receptor might afford too much rigidity. This would suggest the participation of the additional arm of cryptand $\mathbf{L}_3$ in the recognition of the neurotransmitter. Chart 1 depicts possible coordination modes for the prevailing species at physiological pH.

To confirm the high stability obtained for the $\mathbf{L}_3$−dopamine adducts, we have checked the pH-metric stability constants by an alternative UV−vis method. UV spectra of solutions containing a constant amount of $\mathbf{L}_3$ and variable amounts of dopamine at pH 7 show an increase in absorptivity and eventual saturation of an absorption band centered at 214 nm. Fitting of the absorbance vs [Do]/[$\mathbf{L}_3$] plots confirmed the 1:1 Do:$\mathbf{L}_3$ stoichiometry and allowed for the estimation of an effective stability constant of ca. 5 logarithmic units in agreement with the pH-metric studies.

With the purpose of getting additional insight into dopamine complexation, we have performed a NMR study on the formation of dopamine adducts of receptors $\mathbf{L}_2$ and $\mathbf{L}_3$. ^{13}C NMR spectra of dopamine samples with a 3-fold excess of receptors $\mathbf{L}_2$ and $\mathbf{L}_3$ at pH values 6.2 and 7.5 (Table 3; for the labeling of the atoms see drawing of ligands **1**−**3** and Scheme 2) show, as the most noticeable features, downfield shifts for the signals of carbon atoms C3′ and C4′ of the catechol group upon interaction with $\mathbf{L}_2$ and $\mathbf{L}_3$. The shifts are particularly significant at pH 7.5 and are greater for C3 than for C4, which

Table 3. Chemical Shifts ($\Delta\delta$, ppm) Induced in Dopamine (Do) ^{13}C NMR Spectra (D_2O) at pH 6.2 and pH 7.5 by Complexation with **2**[$\mathbf{L}_2$] and **3**[$\mathbf{L}_3$] [Do:L Molar Ratio, 1:3]

dopamine	Do−$\mathbf{L}_2$ pH 6.2	Do−$\mathbf{L}_2$ pH 7.5	**Do**−$\mathbf{L}_3$ pH 6.2	Do−**L3** pH 7.5
Cα′	+0.25	+0.10	+0.08	+0.28
Cβ′	+0.12	+0.08	+0.06	+0.26
C1′	0.0	−0.01	−0.10	−0.02
C2′	+0.06	+0.03	−0.09	−0.09
C3′	+0.20	+0.43	+0.14	+0.65
C4′	+0.19	+0.29	+0.13	+0.58
C5′	+0.07	+0.06	−0.07	+0.13
C6′	−0.05	−0.08	−0.12	−0.14

Table 4. Chemical Shifts ($\Delta\delta$, ppm) Induced in **2**[$\mathbf{L}_2$] and **3**[$\mathbf{L}_3$] ^{13}C NMR Spectra (D_2O) at pH 6.2 and pH 7.5 by Complexation with Dopamine (L:Do Molar Ratio, 1:3)

ligand	$\mathbf{L}_2$−Do pH 6.2	$\mathbf{L}_2$−Do pH 7.5	$\mathbf{L}_3$−Do pH 6.2	$\mathbf{L}_3$−Do pH 7.5
C3,5	+0.23	1.35	+0.30	−1.01
C4	−0.15	+0.56	−0.20	+0.83
C6	+0.08	−0.21	−0.01	−0.01
Cα	−0.07	+0.09	+0.17	−0.11
Cβ	+0.11	−0.55	+0.04	−0.38

may suggest a partial participation of the HDo form in the complexation process.

^{13}C NMR spectra recorded in a 3-fold excess of dopamine with respect to $\mathbf{L}_2$ and $\mathbf{L}_3$ allowed observation of the changes in the receptor signals brought about by dopamine complexation (Table 4). At pH 6.2, the first aspect to be noted is that while the resonance corresponding to carbon atoms C3,5 appears for the free ligands as a broad signal almost embedded in the baseline of the spectra, it sharpens considerably upon addition of dopamine, yielding a broad singlet centered at 141.2 ppm. Moreover, in the case of $\mathbf{L}_3$, C6 presents in the ^{13}C NMR spectrum a signal of anomalous low intensity that becomes notably more intense with the addition of dopamine. All these spectral features provide evidence for the formation of the adducts. In the free receptors, at this pH there would be an interaction between the sp^2 pyrazole nitrogens and the protonated neighboring amine groups that slow the prototropic equilibria of the ring. The formation of the dopamine adducts alters the prototropic exchange rate that becomes remarkably faster. Also, the slight deshielding of the ^{13}C NMR signals of carbons C3,5 and the shielding of C4 denote an increase of the negative charge in the pyrazole ring and agree with the preceding observations (Table 4).

At pH 7.5, the NMR behavior of the pyrazole rings is completely different. Both in the free coronand $\mathbf{L}_2$ and in the free cryptand $\mathbf{L}_3$, the signal of two magnetically equivalent carbons C3,5 are more deshielded and appear as a sharp singlet indicating the absence of interaction with protonated neighboring amine groups. Interaction with dopamine yields shielding and deshielding effects of opposite sign than at pH 6.6, suggesting an increment of positive charge in the pyrazole ring. A plausible explanation for this observation would be a direct interaction of the OH groups of the catechol moiety and the pyrazolic nitrogens. Such an interaction would also be the responsible for the largest shifts of C3′ and C4′ of dopamine observed at this pH (Table 3). The significant shielding of the signals of carbons Cβ of both receptors ($\mathbf{L}_2$, −0.55 ppm; $\mathbf{L}_3$, −0.38 ppm (Table 4)) that occurs at this pH can be ascribed to the simultaneous interaction of dopamine with protonated amine groups close to pyrazole.

As a last aspect in this study, we have modeled the interaction of dopamine with the three receptors with the program MACRO-

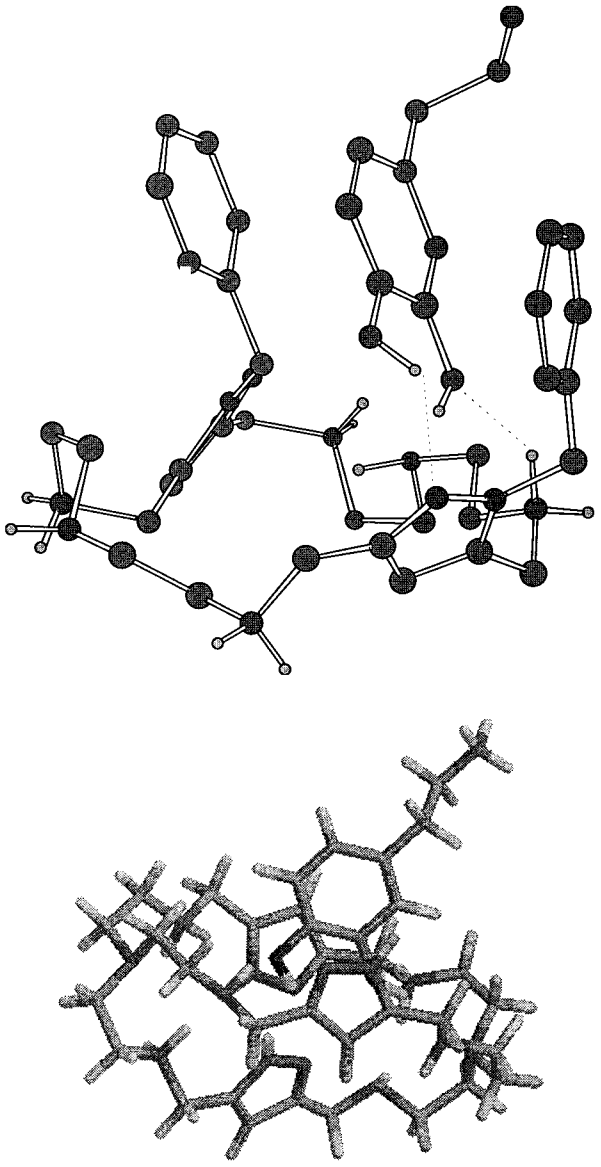

Figure 2. (A, top) Alternative minimum energy conformers for the adduct $H_6\mathbf{L}_1(Do)^{5+}$ ($H_4\mathbf{L}_1{}^{4+}\cdot H_2Do^+$) showing stacking contributions. (B, bottom) Minimum energy conformers for the adduct $H_5\mathbf{L}_3(Do)^{4+}$ ($H_3\mathbf{L}_2\cdot H_2Do^{4+}$).

MODEL 7.0 using AMBER* as a force field.[14a] The hydration energy has been considered with the GB/SA[14b] model incorporated in the MACROMODEL package.

First, a point has to be raised concerning the importance that entropy has in these kind of interactions. Thereby, although the results obtained by models may be corroborative, they can hardly be conclusive.

The family of mimimum energy conformers of the adduct $[H_6\mathbf{L}_1Do]^{5+}$ ($H_4\mathbf{L}_1{}^{4+}\cdot H_2Do^+$) implies structures in which the hydroxyl groups of the catechol fragment are hydrogen bonded to all four protonated amine groups of the receptor close to the pyrazole moiety. Also in several minima of close energy, contributions from stacking interactions between the benzyl groups of the receptor and the dopamine ring can be found (Figure 2A). The minimun energy conformers for $[H_6\mathbf{L}_2Do]^{5+}$ show also that formation of hydrogen bonds between the tetraprotonated receptor and the phenolic groups of the catechol fragment. These data afford some indications that the larger interaction observed for dopamine−$\mathbf{L}_1$ in relation to dopamine−$\mathbf{L}_2$ may be due to additional stacking interactions.

(14) (a) Mohamadi, F.; Richards, N. G. J.; Guida, W. C.; Liskamp, R.; Lipton, M.; Canfield, C.; Chang, G.; Hendickson, T.; Still, W. C. *J. Comput. Chem.* **1990**, *11*, 440. (b) Qiu, D.; Shenkin, P. S.; Hollinger, F. P.; Still, W. C. *J. Phys. Chem.* **1997**, *101*, 3005. (c) Stewart, J. J. P. *J. Comput. Chem.* **1989**, *10*, 209.

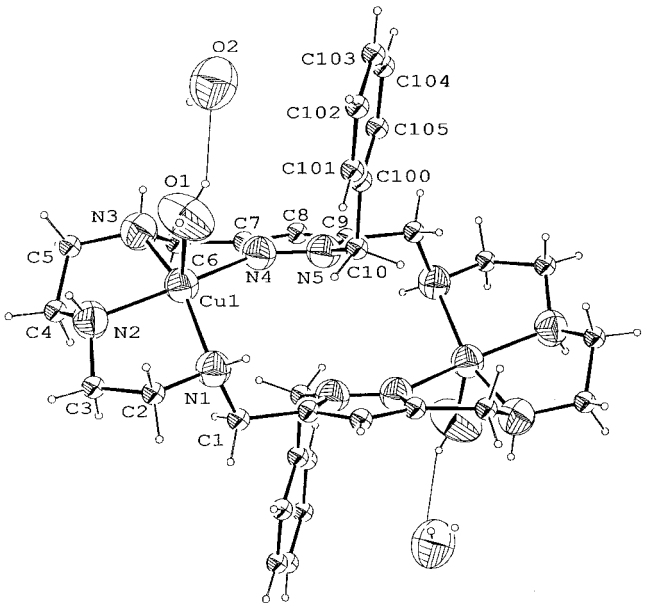

Figure 3. ORTEP drawing for $[Cu_2(\mathbf{L}_1)(H_2O)_2]^{4+}$. Thermal ellipsoids are plotted at the 50% probability level.

The conformational analysis of the cage $\mathbf{L}_3$ is particularly difficult for the many prototropic tautomers that can be present. $[H_5\mathbf{L}_3Do]^{4+}$ ($H_3\mathbf{L}_3{}^{3+}\cdot H_2Do^+$) presents a structure similar to those found for $\mathbf{L}_1$ and $\mathbf{L}_2$ in which different possibilities of formation of hydrogen networks between receptor and substrate are open (Figure 2B). Finally, for $H_6\mathbf{L}_3(Do)^{5+}$ ($H_4\mathbf{L}_3{}^{4+}\cdot H_2Do^+$) the minimum energy structure also reveals the important contribution of hydrogen bonds in the stabilization of the adduct. In some of these structures the participation of the 1H-pyrazole fragment in the hydrogen bond network with the substrate is observed (Figure 2B). None of these structures reveals inclusion of dopamine in the cavity; nevertheless the importance that the entropic term has in these interactions again has to be emphasized, and this parameter could favor an inclusive coordination.

Cu^{2+} Coordination. (a) Crystal Structure of $[Cu_2(\mathbf{L}_1)(H_2O)_2](ClO_4)_4\cdot 2H_2O$ (4). Crystals of the compound $[Cu_2(\mathbf{L}_1)(H_2O)_2](ClO_4)_4\cdot 2H_2O$ (**4**) consists of $[Cu_2(\mathbf{L}_1)(H_2O)]^{4+}$ cations, ClO_4^- anions, and lattice water molecules (Figure 3). Table 5 collects details of the crystal structure refinement and Table 6a selected distances and angles. The coordination geometry around each copper atom is square pyramidal, being the base of the pyramid formed by the three nitrogen atoms of the polyamine bridge [Cu(1)−N(1) = 2.060(3) Å, Cu(1)−N(2) = 2.003(3) Å, Cu(1)−N(3) = 2.027(4) Å, Cu(1)−N(4) = 2.016(3) Å] and the nonbenzylated sp^2 nitrogen of the *N*-benzylpyrazole spacer. The axial position is occupied by a water molecule (Cu(1)−O(1) = 2.170(4) Å). The axial water molecule in each coordination site is hydrogen bonded to another water molecule (O(1)−O(2) = 2.84(1) Å). The copper atom almost resides in the equatorial plane of the pyramid with a mean elevation over the plane defined by the coordinated nitrogen atoms of 0.325(2) Å. The Cu···Cu distance is 6.788(2) Å. The molecule presents an inversion center, and therefore the water molecules are pointing toward opposite sides of the mean plane defined by the macrocyclic cavity. According to those previously observed using

Table 5. Crystallographic Data for **4** and **6**

	4	**6**
empirical formula	$C_{16}H_{27}Cl_2Cu\,N_5O_{10}$	$C_{54}H_{102}Cl_6Cu_4N_{28}O_{28}$
fw	583.87	2058.50
space group	$P2_1/a$	$C2/c$
V, Å^3	2310(2)	8098(5)
a, Å	9.381(5)	44.667(5)
b, Å	19.418(5)	9.124(5)
c Å	12.804(5)	20.050(5)
β, deg	97.931(5)	97.687(5)
T, K	293(2)	293(2)
D_{calcd}, g/cm^3	1.679	1.688
μ(Mo Kα), mm^{-1}	1.24	1.33
2θ range, deg	1−25	1−25
total no. of data	4142	6759
no. of unique data	3902	3411
no. of obsd data[a]	3132	1623
no. of params	326	325
R^b	0.0663	0.0684
$R_w{}^c$	0.1594	0.1776

[a] Observed criterion: $F_o > 4\sigma F_o$. [b] $R_1 = \sum||F_o| - |F_c||/\sum|F_o|$. [c] $R_{w2} = [\sum w(F_o{}^2 - F_c{}^2)/\sum w(F_o)^2]^{1/2}$. For **4**, $w = 1/[\sigma^2(F_o)^2 + (0.10P)^2]$, $P_{max} = (\mathrm{Max}(F_o)^2 + 2(F_c)^2)/3$; for **6**, $w = 1/[\sigma^2(F_o)^2 + (0.14P)^2]$, $P_{max} = (\mathrm{Max}(F_o)^2 + 2(F_c)^2)/3$.

Table 6. Selected Bond Distances (Å) and Bond Angles (deg)

	(a) For Compound **4**		
Cu(1)−N(2)	2.003(3)	N(2)−Cu(1)−N(3)	84.1(1)
Cu(1)−N(4)	2.016(3)	N(4)−Cu(1)−N(3)	80.0(1)
Cu(1)−N(3)	2.027(4)	N(2)−Cu(1)−N(1)	85.6(1)
Cu(1)−N(1)	2.060(3)	N(4)−Cu(1)−N(1)	104.5(1)
Cu(1)−O(1)	2.170(4)	N(2)−Cu(1)−O(1)	98.2(2)
Cu−Cu	6.788(2)	N(4)−Cu(1)−O(1)	98.2(2)
		N(3)−Cu(1)−O(1)	101.6(2)
		N(1)−Cu(1)−O(1)	99.2(2)
	(b) For Compound **6**		
Cu(1)−N(3)	1.90(1)	N(3)−Cu(1)−N(9)	94.7(6)
Cu(1)−N(9)	1.93(2)	N(9)−Cu(1)−N(10)	79.6(6)
Cu(1)−N(10)	2.05(1)	N(3)−Cu(1)−N(2)	81.4(6)
Cu(1)−N(2)	2.11(1)	N(10)−Cu(1)−N(2)	103.7(5)
Cu(1)−N(1)	2.29(2)	N(3)−Cu(1)−N(1)	102.9(6)
Cu(2)−N(8)	1.92(1)	N(9)−Cu(1)−N(1)	111.3(5)
Cu(2)−N(4)	1.92(1)	N(10)−Cu(1)−N(1)	81.4(5)
Cu(2)−N(5)	2.10(1)	N(2)−Cu(1)−N(1)	82.0(5)
Cu(2)−N(7)	2.12(2)	N(8)−Cu(2)−N(4)	94.6(5)
Cu(2)−N(6)	2.40(1)	N(4)−Cu(2)−N(5)	80.2(6)
Cu(1)−Cu(2)	3.960(3)	N(8)−Cu(2)−N(7)	81.4(6)
		N(5)−Cu(2)−N(7)	101.4(7)
		N(8)−Cu(2)−N(6)	105.6(5)
		N(4)−Cu(2)−N(6)	123.7(6)
		N(5)−Cu(2)−N(6)	80.1(4)
		N(7)−Cu(2)−N(6)	81.7(5)

NMR techniques,[11] the benzyl groups are disposed trans to each other, pointing also outward from the macrocyclic cavity.

(b) Crystal Structure of $[Cu_2(H_{-1}L_3)](ClO_4)_3]\cdot 2H_2O$ (6). The crystal structure of **6** consists of $[Cu_2(H_{-1}\mathbf{L}_3)]^{3+}$ cations, ClO_4^- anions, and water molecules. Table 5 presents details of the crystal structure and of the refinement procedure. The coordination geometry around each Cu^{2+} is square pyramidal, the base of the pyramid being formed by two secondary nitrogens of the bridge and two nitrogen atoms of two different pyrazolate moieties which act as exobidentate ligands (Figure 4). The axial positions are occupied by the bridgehead nitrogen atoms, being the distortion more pronounced in one of the two sites [Cu(1)−N(1) = 2.29(2) Å and Cu(2)−N(6) = 2.40(1) Å, Table 6b]. The Cu^{2+}−L distances involving the sp^2 pyrazolate nitrogen atoms [Cu(1)−N(3) = 1.90(1) Å, Cu(1)−N(9) = 1.93(2) Å, Cu(2)−N(4) = 1.92(1) Å, and Cu(2)−N(8) = 1.92(1) Å] are much shorter than those of the secondary nitrogen

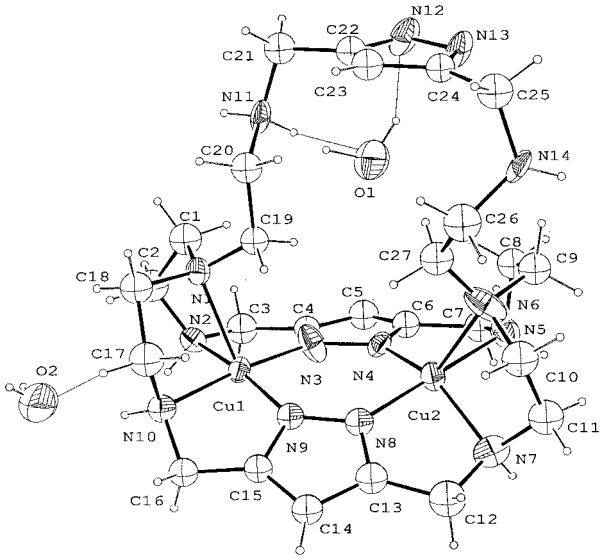

Figure 4. ORTEP drawing of the complex $[Cu_2(H\mathbf{L}_3)](ClO_4)_3]\cdot 2H_2O$. Thermal ellipsoids are plotted at the 50% probability level. ClO_4^- anions are removed for clarity.

atoms [Cu(1)−N(2) = 2.11(1) Å, Cu(1)−N(10) = 2.05(1) Å, Cu(2)−N(5) = 2.10(1) Å, and Cu(2)−N(7) = 2.12(2) Å]. The distance Cu(1)−Cu(2) is 3.960(3) Å. Similar coordination features were observed in the crystal structure of the binuclear complex $[Cu_2(H_{-2}\mathbf{L}_2)](ClO_4)_2$,[12] and in several crystal structures of other pyrazole containing ligands.[6,15] Interestingly enough, we have observed that Cu^{2+} produces the ready deprotonation of the two pyrazole fragments involved in the coordination, without requiring any addition of base (vide infra). However, the pyrazole in the noncoordinating bridge of $\mathbf{L}_3$ (see Figure 4) does not deprotonate, pointing at one side of the macrocyclic cavity. One of the nitrogen atoms of the aliphatic chains is protonated and hydrogen bonded to a water molecule (N(11)−O(1) = 2.79(2) Å) that is placed at one side of the macrocyclic cavity and further connected to the sp^2 nitrogen of the pyrazole group through an additional hydrogen bond (N(12)−O(1) = 3.12(2) Å). The distances of the water molecule to the nonprotonated nitrogen atom of the bridge and to the other pyrazole nitrogen are much longer (5.38 and 3.79 Å, respectively). The other water molecule, placed completely outside of the cavity, is hydrogen bonded to N(10) (N(10)−O(2) = 2.98(2) Å).

The coordination arrangement keeps both Cu^{2+} metal ions close to one face of the cage (the elevation of the Cu atoms over the mean plane defined by the nitrogen donors of the base of the square pyramid are 0.142(7) and 0.272(7) Å for Cu(1) and Cu(2), respectively) leaving enough free room within the cavity for allowing the encapsulation of further substrates as exogenous ligands.

Electromotive Force Measurements. The stability constants for the interaction with Cu^{2+} of receptors $\mathbf{L}_1$−$\mathbf{L}_3$ determined at 298.1 K in 0.15 mol dm^{-3} are presented in Table 7. In all three systems formation of mono- and binuclear complexes is observed. In the system Cu^{2+}−$\mathbf{L}_3$ also a trinuclear species of $[Cu_3(H_{-3}\mathbf{L}_3)]^{3+}$ stoichiometry is even detected.

The thermodynamic data in Table 7 and the distribution diagrams in Figure 5 provide important clues about the coordination characteristics of these pyrazole containing polyaza macrocycles.

(15) (a) Behle, L.; Neuburger, M.; Zehnder, M.; Kaden, T. A. *Helv. Chim. Acta* **1995**, *78*, 693. (b) Weller, H.; Kaden, T. A.; Hopfgartner, G. *Polyhedron* **1998**, *17*, 4543.

Table 7. Stability Constants for the Formation of Cu^{2+} Complexes of Receptors $\mathbf{L}_1$, $\mathbf{L}_2$, and $\mathbf{L}_3$ Determined in 0.15 mol dm^{-3} NaCl at 298.1 K

entry	reaction[a]	$\mathbf{L}_1$	$\mathbf{L}_2$	$\mathbf{L}_3$
1	$Cu + \mathbf{L} + 2H \rightleftharpoons CuH_2\mathbf{L}$	27.9(1)[b]	35.05(2)	35.42(8)
2	$Cu + \mathbf{L} + H \rightleftharpoons CuH\mathbf{L}$	22.13(8)	30.81(2)	29.85(7)
3	$Cu + \mathbf{L} \rightleftharpoons Cu\mathbf{L}$	13.68(6)	23.47(3)	21.76(6)
4	$Cu + \mathbf{L} + H_2O \rightleftharpoons CuH_{-1}\mathbf{L} + H$			13.05(3)
5	$2Cu + \mathbf{L} + H \rightleftharpoons Cu_2H\mathbf{L}$	29.37(5)		39.04(7)
6	$2Cu + \mathbf{L} \rightleftharpoons Cu_2\mathbf{L}$	26.27(3)	34.45(3)	36.72(3)
7	$2Cu + \mathbf{L} \rightleftharpoons Cu_2H_{-1}\mathbf{L} + H$	16.85(4)		31.31(5)
8	$2Cu + \mathbf{L} \rightleftharpoons Cu_2H_{-2}\mathbf{L} + 2H$	7.06(3)	26.56(3)	24.13(5)
9	$3Cu + \mathbf{L} \rightleftharpoons Cu_3H_{-3}\mathbf{L} + 3H$			25.78(4)
10	$CuH\mathbf{L} + H \rightleftharpoons CuH_2\mathbf{L}$	5.8	4.2	6.6
11	$Cu\mathbf{L} + H \rightleftharpoons CuH\mathbf{L}$	8.5	7.3	7.1
12	$Cu\mathbf{L} \rightleftharpoons CuH_{-1}\mathbf{L} + H$			−8.7
13	$Cu\mathbf{L} + Cu \rightleftharpoons Cu_2\mathbf{L}$	12.6	11.0	15.0
14	$Cu_2\mathbf{L} + H \rightleftharpoons Cu_2H\mathbf{L}$	3.1		2.3
15	$Cu_2\mathbf{L} \rightleftharpoons Cu_2H_{-1}\mathbf{L} + H$	−9.4		−5.4
16	$Cu_2H_{-1}\mathbf{L} \rightleftharpoons Cu_2H_{-2}\mathbf{L} + H$	−9.8		−7.2
17	$Cu_2\mathbf{L} \rightleftharpoons Cu_2H_{-2}\mathbf{L} + 2H$	−19.2	−7.9	−12.6

[a] Charges omitted for clarity. [b] Values in parentheses are standard deviations in the last significant figure.

The speciation shows for the three systems the formation of the mononuclear species $[CuH_2L]^{4+}$, $[CuHL]^{3+}$, and $[CuL]^{2+}$; for the system $Cu^{2+}-\mathbf{L}_3$ also the species $[CuH_{-1}\mathbf{L}_3]^{+}$ was observed. The most important difference between the three systems is the much lower constants obtained for the benzylated receptor $\mathbf{L}_1$ with respect to $\mathbf{L}_2$ and $\mathbf{L}_3$; the formation constant for the $[Cu\mathbf{L}_1]^{2+}$ species is 13.68 logarithmic units, while those for the corresponding species of $\mathbf{L}_2$ and $\mathbf{L}_3$ are over 20 logarithmic units (entry 3 in Table 7). This situation can be ascribed to the fact that the benzylated receptor is unable to deprotonate and yield the stronger field pyrazolate ligand. UV−vis spectra are not very clear in identifying this situation since formation of the binuclear complexes is even detected for low Cu^{2+}:**L** metal ratios (see Figure 5). On the other hand, the large protonation constants of the $[CuL]^{2+}$ complexes (entry 11) denotes that these processes are ocurring in non-coordinated nitrogen atoms of the three receptors.

The thermodynamic data for the binuclear $Cu^{2+}-\mathbf{L}_1$ complexes agree well with the fundamental coordination characteristics evidenced by the crystal structure (vide supra). Indeed in this case, both coordination sites seem to act almost independently. The stepwise addition of the second Cu^{2+} ion displays a constant almost as high as that of the addition of the first metal ion (entries 13 and 3 in the table, respectively). Furthermore, the hydrolysis of the water molecules in the binuclear complex $[Cu_2\mathbf{L}_1]^{4+}$ to give the hydroxo species present pK_a values close between them (9.4 and 9.8, entries 15 and 16) and high enough to discard the formation of hydroxo bridges between the copper(II) metal ions.

In view of these thermodynamic parameters and of the X-ray study previously discussed, the structures in Chart 2 can be proposed for the three main binuclear species in solution for a molar Cu:$\mathbf{L}_1$ ratio 2:1. $[Cu_2(\mathbf{L}_1)(H_2O)_2]^{4+}$ would be coincident with the X-ray structure, while all the data strongly suggest that neither in $[Cu_2(\mathbf{L}_1)(H_2O)(OH)]^{3+}$ nor in $[Cu_2(\mathbf{L}_1)(OH)_2]^{2+}$ is there formation of hydroxo bridges between the metal centers.

The distribution diagram of the system $Cu^{2+}-\mathbf{L}_2$ in molar ratio 2:1 shows the formation of $[Cu_2H_{-2}\mathbf{L}_2]^{2+}$ as the unique species in solution above pH 4.5. The formation of this species implies the deprotonation of the two pyrazole spacers that according to the X-ray structure[12] will be acting as exobidentate bridging ligands between both metal centers. As shown by the constants (entries 8 and 17 in Table 7), these deprotonation processes occur cooperatively, and as a consequence we could not calculate a constant for the first one. The binuclear $[Cu_2H_{-2}\mathbf{L}_2]^{2+}$ species are the main ones in solution even for low metal:ligand molar ratios (see Figure 5). Therefore, Cu^{2+}

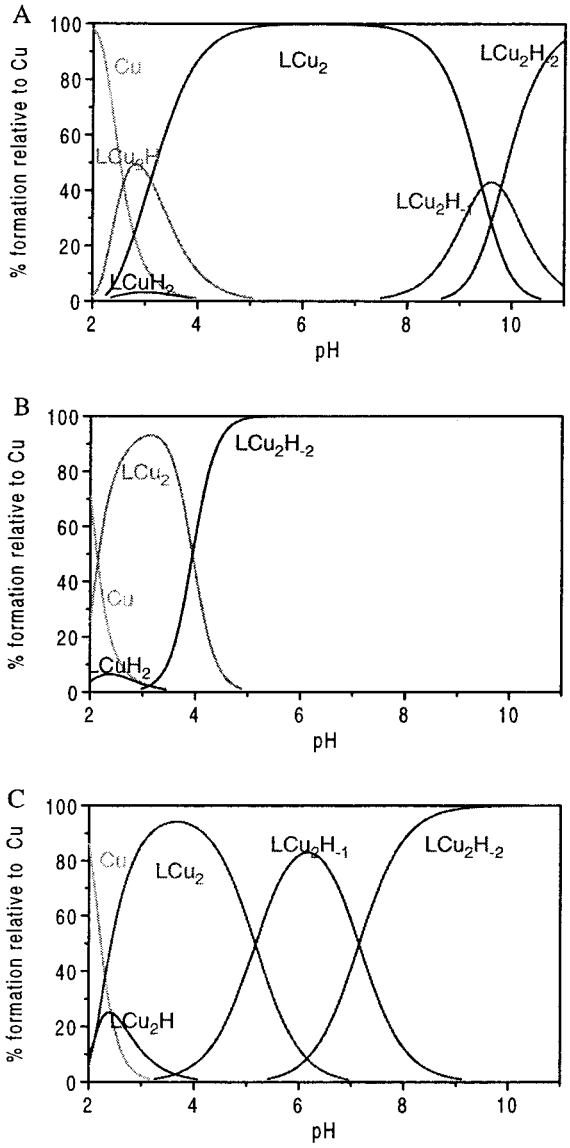

Figure 5. Distribution diagram for the systems (A) $Cu^{2+}-\mathbf{L}_1$, (B) $Cu^{2+}-\mathbf{L}_2$, and (C) $Cu^{2+}-\mathbf{L}_3$, calculated for molar ratios 2:1 Cu^{2+}:**L** ($[Cu^{2+}] = 2 \times 10^{-3}$ mol dm^{-3}).

Chart 2

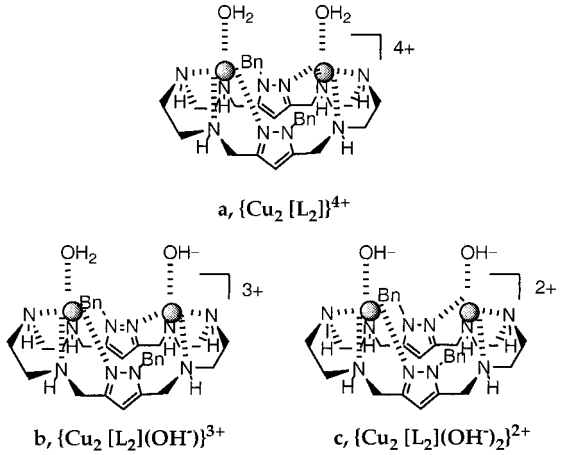

coordination promotes a dramatic increase of the acidity of the pyrazole fragment than when free does not deprotonate up to pH 12.[11] Also the cooperative behavior of both coordination sites in $\mathbf{L}_2$ should be noted.

Deprotonation of the pyrazole units in aqueous solution induced by coordination to metal is a characteristic feature of this heterocycle. Kaden et al.[15] have evidenced this behavior in the Cu^{2+} complexes of a bis(macrocyclic) receptor containing two 1,4,7-triazacyclononane ([9]aneN$_3$) unit connected to the 3,5 positions of a pyrazole spacer through methylenic groups ($\mathbf{L}_5$).[15] Deprotonation of the 1H-pyrazole group in the $[Cu_2\mathbf{L}_5]^{4+}$ complex presented a pK_a value of 3.67 that falls in the range of the values here reported (Table 7). Similar conclusions were derived for these authors for a related bis(macrocyclic) ligand with 1,4,7-azadithianonane ([9]aneNS$_2$) units.[15b]

In a previous paper some of us[12] reported on the crystal structure of complex **4**. In such a structure both pyrazole units were deprotonated, behaving as bis(bidentate) anions. The crystals were grown from an ethanolic solution of the ligand to which 2 mol of NaOH/(mol of ligand) were added. Here, we have arrived at the same complex without the addition of base following a re-crystallization in water (see Experimental Section). This experiment gives further support to the ready deprotonation that the pyrazole groups experience in aqueous solution induced by the presence of metal ions.

The stability data for the mono- and binuclear Cu^{2+} complexes of the cryptand $\mathbf{L}_3$ shows similarities with those discussed for the system $Cu^{2+}-\mathbf{L}_2$. The greatest differences between the two systems are the larger stability of the $[Cu_2\mathbf{L}_3]^{4+}$ complex with respect to $[Cu_2\mathbf{L}_2]^{4+}$ and the reduced acidity of the pyrazole moeities in the binuclear Cu^{2+} complexes of $\mathbf{L}_3$ (pK_{a1} = 5.4, pK_{a2} = 7.2, entries 15 and 16 in Table 7; see Figure 5). While, for $\mathbf{L}_2$, the two pyrazole moieties are already fully deprotonated at pH 5, for $\mathbf{L}_3$ such a situation seems to be only achieved at pH 8.5. Probably, the presence of the additional bridge in the cryptand structure can contribute to make more rigid the molecule, disrupting somewhat the cooperativity observed in $\mathbf{L}_2$ for these processes.

A final point that deserves some comment is the formation of a trinuclear $[Cu_3\mathbf{L}_3H_{-3}]^{3+}$ complex (Table 7, entry 9) which is the species majoritary in solution for molar ratios 3:1 Cu^{2+}:$\mathbf{L}_3$ over pH 5. The formation of this complex should imply the deprotonation of all three pyrazole fragments of the cage at a relatively low pH value. Currently we are performing experiments to try to unravel the molecular structure of this complex.

Mixed Complexes $Cu^{2+}-$L-Dopamine. The formation of mixed complexes $Cu^{2+}-$L-dopamine has been followed by potentiometric measurements at 298.1 K in 0.15 mol dm^{-3} NaCl using molar ratios $Cu^{2+}-$L-dopamine ranging from 2:1:1 to 2:1:3. The model species and stability constants that best fit the experimental data correspond to the formation of ternary complexes with stoichiometries $Cu^{2+}-$L-dopamine 2:1:1. The stability constants for such systems are included in Table 8. The distribution diagrams for the three systems calculated for molar ratios 1:2:1 Cu^{2+}:**L**:dopamine are reported in Figure 6.

These ternary complexes are for $\mathbf{L}_2$ only the main species in solution above pH 8.5 in correspondence with the formation of the species $[Cu_2(H_{-2}\mathbf{L}_2)(DoH)]^{2+}$ and $[Cu_2(H_{-2}\mathbf{L}_2)(Do)]^{+}$. However, in the case of $\mathbf{L}_1$ the mixed complexes are always the main ones in solution prevailing throughout the entire pH range studied (pH 3−11). This behavior can find its explanation in the different nature of the binuclear complexes formed. As discussed previously, for $\mathbf{L}_2$, the coordination sites of the Cu^{2+} ions were made up by five nitrogen donors, occupying the central nitrogens of the diethylenetriamine subunits in the axial positions of the square pyramid. Formation of mixed complexes requires the detachment of at least one of the nitrogen donors (most likely the one in the axial position), and this would be

Table 8. Stability Constants for the Formation of $Cu^{2+}-\mathbf{L}-$Do Complexes of Receptors $\mathbf{L}_1$, $\mathbf{L}_2$, and $\mathbf{L}_3$ (Do = Dopamine) Determined in 0.15 mol dm^{-3} NaCl at 298.1 K

entry	reaction[a]	$\mathbf{L}_1$	$\mathbf{L}_2$	$\mathbf{L}_3$
1	$2Cu + \mathbf{L} + Do + 2H \rightleftharpoons Cu_2H_2\mathbf{L}Do$	49.01(4)[b]		59.6(1)
2	$2Cu + \mathbf{L} + Do + H \rightleftharpoons Cu_2H\mathbf{L}Do$	42.15(6)	51.7(2)	54.2(1)
3	$2Cu + \mathbf{L} + Do \rightleftharpoons Cu_2\mathbf{L}Do$			47.0(1)
4	$2Cu + \mathbf{L} + Do \rightleftharpoons Cu_2H_{-1}\mathbf{L}Do + H$	26.20(4)	40.56(3)	38.5(1)
5	$2Cu + \mathbf{L} + Do \rightleftharpoons Cu_2H_{-2}\mathbf{L}Do + 2H$	18.40(4)	30.36(4)	
6	$2Cu + \mathbf{L} + Do \rightleftharpoons Cu_2H_{-3}\mathbf{L}Do + 3H$	8.19(4)		
8	$Cu_2L + H_2Do \rightleftharpoons Cu_2H_2\mathbf{L}Do$	3.5		3.6
9	$Cu_2H_{-1}\mathbf{L} + H_2Do \rightleftharpoons Cu_2H\mathbf{L}Do$	6.2		3.9
10	$Cu_2\mathbf{L} + HDo \rightleftharpoons CuH\mathbf{L}Do$	5.6		
11	$Cu_2H_{-2}\mathbf{L} + HDo \rightleftharpoons CuH_{-1}\mathbf{L}Do$	8.8	3.7	4.0
12	$Cu_2H_{-2}\mathbf{L} + Do \rightleftharpoons CuH_{-2}\mathbf{L}Do$	11.3	3.8	

[a] Charges omitted for clarity. [b] Values in parentheses are standard deviations in the last significant figure.

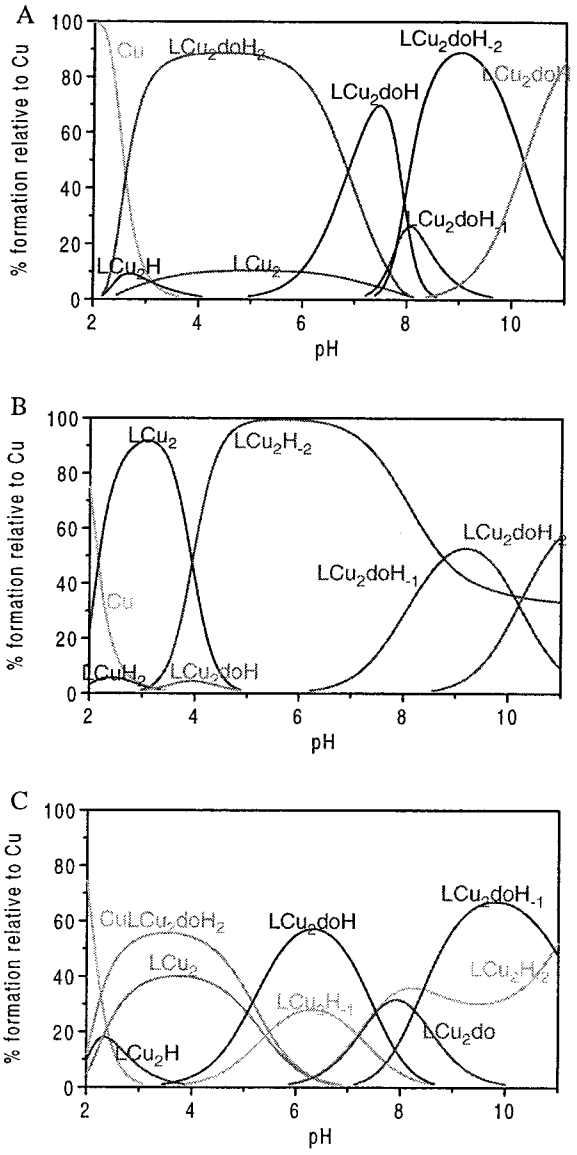

Figure 6. Distribution diagram for the systems (A) $Cu^{2+}-\mathbf{L}_1-$Do, (B) $Cu^{2+}-\mathbf{L}_2-$Do, and (C) $Cu^{2+}-\mathbf{L}_3-$Do, calculated for molar ratios 2:1:1 Cu^{2+}:**L**:Do ($[Cu^{2+}] = 2 \times 10^{-3}$ mol dm^{-3}).

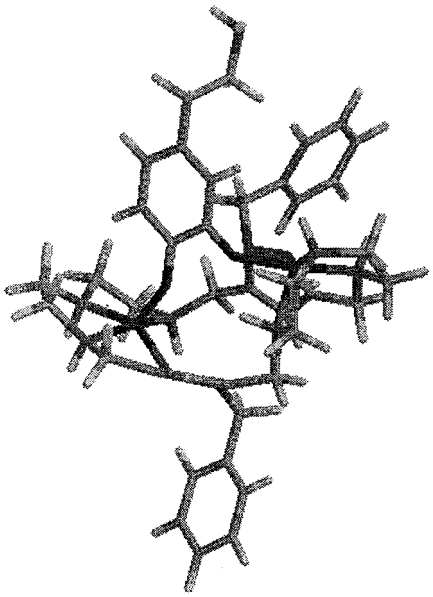

Figure 7. Model for the formation of ternary complexes $Cu^{2+}-\mathbf{L}_1-$Do.

only efficient when the hydroxo groups of dopamine deprotonate to bind the Cu^{2+} ions at around pH 8.

For $\mathbf{L}_1$, however, the axial positions in the first coordination sphere are occupied by labile water molecules, which are more easily replaced by catecholamine favoring the formation of the ternary species. Although it is difficult to advance an hypothesis on structural aspects of the mixed complexes, the stoichiometries found and initial molecular modeling studies performed with the program SPARTAN[14c] suggest the possibility that dopamine could act as a bridging exogenous ligand between both coordination sites. Cu^{2+} coordination would be facilitating the partial deprotonation of the phenolic groups (Figure 7).

For the system $Cu^{2+}-\mathbf{L}_3-$dopamine formation of mixed complexes is observed throughout all of the pH range investigated. These species display intermediate stabilities between those of the ternary complexes of $\mathbf{L}_1$ and $\mathbf{L}_2$. Although the coordination arrangement around the Cu^{2+} ions in the binary complexes of $\mathbf{L}_2$ and $\mathbf{L}_3$ is similar, inclusion of dopamine in the void upper part of the cavity might contribute to the larger stability of the $\mathbf{L}_3$ ternary complexes.

Chart 3 shows possible coordination modes for the ternary complexes prevalent around physiological pH.

Chart 3

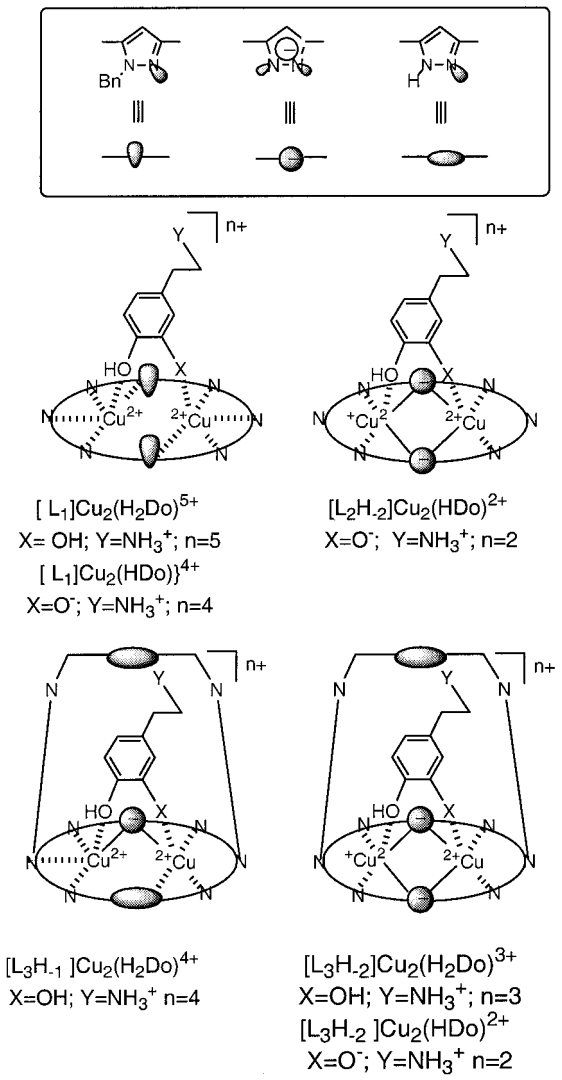

Conclusions

The results analyzed show that cryptand $\mathbf{L}_3$ is a particularly well-suited receptor for dopamine recognition in aqueous solution. All three receptor form very stable binuclear Cu^{2+} complexes in aqueous solution. Formation of the Cu^{2+} complexes induces the ready deprotonation of the pyrazole units in $\mathbf{L}_2$ and $\mathbf{L}_3$. Crystal structures of the complex $[Cu_2(\mathbf{L}_1)(H_2O)_2](ClO_4)_4 \cdot 2H_2O$ (**4**) denote the participation of the sp^2 nitrogen donors of the nonbenzylated *N*-benzylpyrazole nitrogen donors in the coordination of the Cu^{2+} metal ions which present square pyramidal geometry with a water molecule in axial position (Figure 3). The crystal structure of $[Cu_2(H_{-1}\mathbf{L}_3)](ClO_4)_3]\cdot 2H_2O$ (**6**) shows also square pyramidal coordination geometry around each Cu^{2+}. The axial positions are occupied in this case by the bridgehead nitrogen of the cage. The two deprotonated pyrazole subunits behave as exobidentate ligands. In this structure there is a water molecule strongly retained by hydrogen bonds with a protonated amine group and the nondeprotonated pyrazole of the bridge that does not participate in the coordination to the metal. Solution studies agree with the fundamental characteristic denoted by the crystal structures and also suggest the possible formation of trinuclear species for $\mathbf{L}_3$.

Formation of ternary complexes $Cu^{2+}-$dopamine$-\mathbf{L}$ is particularly relevant in the case of $\mathbf{L}_1$ where most likely the hydroxyl groups of the catechol would be replacing the axially coordinated water molecules.

The results here presented give interesting perspectives for the design of receptors for neurotransmitters. Currently we are exploring these insights.

Experimental Section

The starting materials were purchased from commercial sources and used without further purification. The solvents were dried using standard techniques. All reactions were monitored by thin-layer chromatography using DC-Alufolien silica gel $60PF_{254}$ (Merck; layer thickness, 0.2 mm). Compounds were detected with iodine or with phosphomolybdic acid reagent. Melting points were determined in a Reichert−Jung hot-stage microscope and are uncorrected. ^{1}H and ^{13}C NMR spectra were recorded on Varian Unity Inova-400 and Varian Unity-500 spectrometers. The chemical shifts are reported in parts per million from tetramethylsilane but were measured against the solvent signals; dioxane ($\delta = 67.4$ ppm) was used as reference for ^{13}C NMR spectra in D_2O. All assignments

have been performed on the basis of $^1H-^{13}C$ heteronuclear multiple quantum coherence experiments (HMQC, HMBC, GHMQC, and GHMBC). In the NMR study of the complexation of ligands with dopamine, the pH was calculated from the measured pD values using the correlation pH = pD − 0.4.[16] UV−vis spectra were recorded with a Perkin-Elmer Lambda 9 spectrophotometer. FAB mass spectra were obtained on a VG AutoSpec spectrometer using a *m*-nitrobenzyl alcohol matrix. Elemental analyses were provided by the Departamento de Análisis, Centro de Química Orgánica "Manuel Lora Tamayo", CSIC, Madrid, Spain.

Preparation of Ligands 1−3. Ligands **1** (L_1) and **2** (L_2) were prepared by reaction of the corresponding 3,5-pyrazoledicarbaldehydes with diethylenetriamine as reported previously.[17]

(a) 1,4,7,8,11,14,17,20,21,24,29,32,33,36-Tetradecaazapentacyclo-[12.12.12.1^{6,9}.1^{19,22}.1^{31,34}]hentetraconta-6,9(41),19(40),21,31,34(39)-hexaene (3) [L_3]. 3,5-Pyrazoledicarbaldehyde[11] (0.228 g, 6 mmol) was dissolved in warm methanol (120 mL) and added dropwise during 2 h and under an argon atmosphere to a stirred solution of tris(2-aminoethyl)amine (0.292 g, 2 mmol) in methanol (80 mL). After stirring overnight at room temperature, sodium borohydride (228 mg, 6 mmol) was added portionwise, and after 2 h the solvent was evaporated to dryness under reduced pressure. The residue was directly recrystallized from water (15 mL), and the obtained crystals, after drying under vacuum at 80 °C over phosphorus pentoxide, were shown to be the title compound as the monohydrate (0.380 g, 65%); mp 245 °C. ^1H NMR (400 MHz, CD_3OD): δ 6.24 (s, 3 H, H_4), 3.88 (s, 12 H, H_6), 2.90−2.93 (m, 12 H, H_α), 2.78−2.81 (m, 12 H, H_β). ^{13}C NMR (100 MHz, CD_3OD): δ 147.92 (br s, $C_{3,5}$), 103.28 (C_4), 54.86 (C_β), 48.54 (C_α), 46.47 (C_6). FAB-MS (*m*/*z*, %): 569 $[M + H]^+$ (60), 307 (17), 154 (100), 136 (83). Anal. Calcd (%) for $C_{27}H_{48}N_{14}\cdot H_2O$ (586.8): C, 55.27; H, 8.59; N, 33.42. Found: C, 55.42; H, 8.91; N, 33.70.

Compounds **2** and **3** decompose partially after some time; although they can be easily purified by recrystallization from toluene or water, respectively, it is preferable to store them as the corresponding hydrochlorides, prepared as follows: A mixture of the corresponding ligand (**2** or **3**) (0.5 mmol) and 1 M aqueous hydrochloric acid (4 mL) was stirred for 12 h. After addition of ethanol (50 mL), the crystallized white solid was isolated by filtration and dried over phosphorus pentoxide at 60 °C.

(b) Compound 2·6HCl·2H$_2$O. Yield 0.294 g (91%); mp 250−252 °C. ^1H NMR (400 MHz, D_2O): δ 6.67 (s, 2 H, H_4), 4.31 (s, 8 H, H_6), 3.38 (t, ^3J(H,H) = 6.8 Hz, 8 H, H_β), 3.28 (t, ^3J(H,H) = 6.8 Hz, 8 H, H_α). ^{13}C NMR (100 MHz, D_2O): δ 139.74 ($C_{3,5}$), 110.30 (C_4), 44.99 (C_β), 43.88 (C_6), 43.00 (C_α). Anal. Calcd (%) for $C_{18}H_{34}N_{10}\cdot 6HCl\cdot 2H_2O$ (645.3): C, 33.50; H, 6.87; N, 21.70. Found: C, 33.90; H, 6.89; N, 21.94.

(c) Compound 3·8HCl·2H$_2$O. Yield 0.399 g (89%); mp 266−269 °C. ^1H NMR (500 MHz, D_2O): δ 6.59 (s, 3 H, H_4), 4.27 (s, 12 H, H_6), 3.31 (t, ^3J(H,H) = 5.6 Hz, 12 H, H_α), 2.78 (t, ^3J(H,H) = 5.6 Hz, 12 H, H_β). ^{13}C NMR (125 MHz, D_2O): δ 140.32 ($C_{3,5}$), 109.88 (C_4), 51.25 (C_β), 46.24 (C_α), 44.58 (C_6). Anal. Calcd (%) for $C_{27}H_{48}N_{14}\cdot 8HCl\cdot 2H_2O$ (896.5): C, 36.17; H, 6.75; N, 21.87. Found: C, 36.40; H, 7.00; N, 22.02.

Preparation of Cu^{2+} Binuclear Complexes 4−6. Working under an argon atmosphere, a solution of $Cu(ClO_4)_2\cdot 6H_2O$ (74 mg, 0.2 mmol) in anhydrous methanol (1 mL) was dropped with stirring to another of the corresponding ligands **1**−**3** [L_1-L_3] (0.1 mmol) in the same solvent (2 mL). After 12 h, the precipitated blue solid was collected by filtration and vacuum-dried at 100 °C over phosphorus pentoxide. Slow evaporation at room temperature of a solution of the obtained complexes in boiling water (10 mL) afforded crystals suitable for elemental and X-ray diffraction analysis.

(a) [Cu$_2$(L$_1$)(H$_2$O)$_2$](ClO$_4$)$_4$·2H$_2$O (4). Yield 84 mg (74%); mp >350 °C. FAB-MS (*m*/*z*, %): 995 $[M + 2 - ClO_4]^+$ (4), 896 $[M + 2 - 2ClO_4]^+$ (9), 795 $[M - 3ClO_4]^+$ (12). Anal. Calcd (%) for $C_{32}H_{46}Cl_4Cu_2N_{10}O_{16}\cdot 2H_2O$ (1131.7): C, 33.96; H, 4.45; N, 12.38. Found: C, 34.15: H, 4.59; N, 12.61.

(b) [Cu$_2$(H$_{-2}$L$_2$)](ClO$_4$)$_2$ (5). Yield 59 mg (83%); mp >350 °C. FAB-MS (*m*/*z*, %): 614 $[M + 1 - ClO_4]^+$ (10), 514 $[M - 2ClO_4]^+$ (10). Anal. Calcd (%) for $C_{18}H_{32}Cl_2Cu_2N_{10}O_8$ (714.5): C, 30.26; H, 4.51; N, 19.60. Found: C, 29.88; H, 4.65; N, 19.35.

(c) [Cu$_2$(H$_{-1}$L$_3$)](ClO$_4$)$_3$·2H$_2$O (6). Yield 81 mg (79%); mp >350 °C. FAB-MS (*m*/*z*, %): 893 $[M + 2 - ClO_4]^+$ (1), 793 $[M + 1 - 2ClO_4]^+$ (12), 692 $[M - 1 - 3ClO_4]^+$ (10). Anal. Calcd (%) for $C_{27}H_{47}Cl_3Cu_2N_{14}O_{12}\cdot 2H_2O$ (1029.2): C, 31.51; H, 4.99; N, 19.05. Found: C, 31.88; H, 4.83; N, 18.87.

Electromotive Force Measurements. The potentiometric titrations were carried out in 0.15 M NaCl at 298.1 ± 0.1 K by using the experimental procedure (buret, potentiometer, cell, stirrer, microcomputer, etc.) that has been fully described elsewhere.[17] The acquisition of the electromotive force (emf) data was performed with the computer program PASAT.[18] The reference electrode was a Ag/AgCl electrode in saturated KCl solution. The glass electrode was calibrated as a hydrogen ion concentration probe by titration of well-known amounts of HCl with CO_2-free NaOH solutions[19] and determination of the equivalent point by Gran's method,[20] which gives the standard potential $E^{\circ\prime}$ and the ionic product of water [pK_w = 13.73(1)]. The computer program HYPERQUAD[21] was used to calculate the protonation and stability constants, and the DISPO[22] program was used to obtain the distribution diagrams. The titration curves for each system (ca. 200 experimental points corresponding to at least three measurements, pH 2−11, concentration of ligands $1 \times 10^{-3}-5 \times 10^{-3}$ M) were treated either as a single set or as separated curves without significant variations in the values of the stability constants. Finally, the sets of data were merged together and treated simultaneously to give the final stability constants.

X-ray Structure Analysis. Analysis on single crystals of the ligands were carried out with an Enraf-Nonius CAD-4 single-crystal diffractometer (λ = 0.710 69 Å). The unit cell dimensions were measured from the angular settings of 25 reflections with θ between 5 and 25°. The space groups were $P2_1/a$ and $C2/c$, for **4** and **6**, respectively. A total of 4142 and 6759 reflections were measured in the *hkl* range (0, 0, −12) to (11, 23, 15) and (0, −10, 0) to (52, 10, 23) between θ limits $1.61 < \theta < 25.00°$ and $1.84 < \theta < 24.97°$. $\omega-2\theta$ scan techniques and a variable scan rate with a maximum scan time of 60 s per reflection were used. The intensity of the primary beam was checked throughout the data collection by monitoring three standard reflections every 3600 s. Profile analysis was performed on all reflections;[23] a semiempirical absorption correction, Ψ-scan based, was performed.[24] For **4** and **6** respectively a total of 3902 and 3411 "unique" reflections from which 3132 and 1623 were with $F_o > 4\sigma(F_o)$. Lorenz and polarization corrections were applied, and the data were reduced to $|F_o|$ values. The structure was solved by the Patterson method using the program SHELXS-86,[25] running on a Pentium 100 computer. Isotropic least-squares refinement was performed by means of the program SHELXL-93,[26] converging to R = 0.10; at this stage an additional empirical absorption correction was applied using DIFABS.[27] The maximum and minimum absorption correction factors were 0.92 and 1.21. Hydrogen atoms were geometrically placed. Table 5 presents details of the crystal data.

(16) Covington, A. K.; Paabo, M.; Robinson, R. A.; Bates, R. G. *Anal. Chem.* **1968**, *40*, 700.

(17) García-España, E.; Ballester, M. J.; Lloret, F.; Moratal, J.-M.; Faus, J.; Bianchi, A. *J. Chem. Soc., Dalton Trans*. **1988**, 101.

(18) Fontanelli, M.; Micheloni, M. *Proceedings of the 1st Spanish−Italian Congress on Thermodynamics of Metal Complexes*; Disputación de Castellón: Peñíscola, Castellón, Spain, June, 3−6, 1990.

(19) Micheloni, M.; Sabatini, A.; Vacca, A. *Inorg. Chim. Acta* **1977**, *25*, 41.

(20) (a) Gran, G. *Analyst (London)* **1952**, *77*, 661. (b) Rossoti, F. J. C.; Rossoti, H. *J. Chem. Educ.* **1965**, *42*, 375.

(21) Gans, P.; Sabatini, A.; Vacca, A. *Talanta* **1996**, *43*, 1739.

(22) Vacca, A. *DISPO*; a FORTRAN program for the determination of species distribution in multicomponent systems, 1984.

(23) Lehman, M. S.; Larsen, F. K. *Acta Crystallogr., Sect. A* **1978**, *30*, 580. Grant, D. F.; Gabe, E. J. *J. Appl. Crystallogr., Sect. A* **1978**, *11*, 114.

(24) Nort, A. C. T.; Philips, D. C.; Mathews, F. S. *Acta Crystallogr., Sect. A* **1978**, *11*, 114.

(25) Sehldrick, G. M., Kruger, C., Goddard, R., Eds. *Crystallographic Computing*; Clarendon Press: Oxford, England, 1985; p 175.

(26) Sehldrick, G. M. *SHELXS-93: Program for Crystal Structure Refinement*; Institute für Anorganische Chemie der Universitat, Göttingen: Göttingen, Germany, 1993.

(27) Walker, N.; Stuart, D. *Acta Crystallogr. Sect. A* **1983**, *39*, 158.

During the final stages of the refinement the positional parameters and the anisotropic thermal parameters of the non-hydrogen atoms were refined. The hydrogen atoms were refined with a common thermal parameter. The final conventional agreement factors for **4** and **6** were respectively $R_1 = 0.0663$, $R_{w2} = 0.1594$ and $R_1 = 0.0684$, $R_{w2} = 0.1776$. Atomic scattering factors were taken from the ref 28. Molecular plots were produced by the program ORTEP.[29]

Molecular Mechanics Calculations. Molecular mechanics calculations were performed with MACROMODEL 7.0 package using AMBER*[14a] as force-field and GB/SA[14b] solvation model for water.

Semiempirical calculations of the metal complex structures were performed with PC SPARTAN PRO 1.0.5 using the PM3 parametrization.[14c]

(28) *International Tables for X-ray Crystallography*; Kynoch Press: Birmingham, England, 1974.

(29) Johnson, C. K. *ORTEP*; Report ORNL-3794; Oak Ridge National Laboratory: Oak Ridge, TN, 1971.

Acknowledgment. This work is devoted to the memory of Prof. Dr. José Antonio Ramírez Belenguer. Financial support by the Spanish "Comisión Interministerial de Ciencia y Tecnología" (CICYT, Projects SAF-96-0242-CO2-01, SAF-99-0063, and BQU2000-1424-CO3) is gratefully acknowledged.

Supporting Information Available: Crystal data and structure refinement details (Tables S1 and S1′), atomic coordinates (Table S2 and S2′), bond lengths and angles (Table S3 and S3′), anisotropic displacement parameters (Tables S4 and S4′), and hydrogen coordinates for **4** and **6** (Tables S5 and S5′) (PDF). This material is available free of charge via the Internet at http://pubs.acs.org.

JA010956P